

# Research Journal of Pharmaceutical, Biological and Chemical Sciences

## X-ray Diffraction Analysis of Silicon Nanoparticles and Nanowires.

R. B. Assilbayeva<sup>1</sup>, A. Yu. Kharin<sup>2</sup>, J. V. Kargina<sup>2,3</sup>, A. Zh. Turmukhamedov<sup>1</sup>, and V. Yu. Timoshenko<sup>2,3\*</sup>.

<sup>1</sup> Satpaev National Research Kazakh University, 050013 Almaty, Kazakhstan.

<sup>2</sup> National Research Nuclear University MEPhI, 115409 Moscow, Russia.

<sup>3</sup> Lomonosov Moscow State University, Physics Department, 119991 Moscow, Russia.

### ABSTRACT

Nanoparticles (NPs) and nanowires (NWs) of chemically pure silicon (Si) were investigated by means of x-ray diffraction (XRD) technique. Broadening of the XRD lines of crystalline Si lattice was used to estimate the mean size of Si NPs. Silicon nanoparticles were found to decrease their sizes due to dissolution process in water for several days. The dissolution rate was found to be dependent on the morphology of Si nanoparticles and their surface coating. The obtained results can be useful for biomedical and sensor applications of Si-based nanostructures.

**Keywords:** nanoparticles, nanowires, silicon, oxidation, x-ray, diffraction.

*\*Corresponding author*

## INTRODUCTION

Silicon (Si) nanostructures have attracted a lot of interest since the discovery of visible photoluminescence from porous silicon (PSi) [1]. Si-based nanostructures have been considered for optoelectronics [2], photovoltaics [3,4], and various sensor [5,6] applications. Furthermore, it has been demonstrated a large panel of imaging and therapeutic modalities, including theranostic applications of Si nanoparticles (NPs) [7-9]. It was found that small Si NPs can be dissolved in water and aqueous solutions [10]. While the dissolution rate of bulk crystalline silicon (c-Si) is defined by the solution pH and orientation of monocrystalline surface, the dissolution rate of NPs mainly depends on their size, morphology and surface oxide coating. Despite of numerous different parameters, the most important dependence is that the small Si NPs are degraded into water solution during relatively short times (up to 24 h). The fact of fast degradation of Si NPs leads to arise of the huge number of research on application of PSi NPs for drug delivery and controlled drug release [8]. Nevertheless, the control on the dissolution rate without changing the size of particles will be very helpful for the bio-applications of Si NPs. In the present paper we show the possibility to monitor the mean size and dissolution rate of Si NPs by means of the XRD technique.

## MATERIALS AND METHODS

Samples of microporous silicon were formed by standard method of the electrochemical etching [1,2] of bulk c-Si wafers (p-type, boron doped to the specific resistance of 1-10  $\Omega\cdot\text{cm}$ , (100)- oriented) in a mixture of hydrofluoric acid (48%) and ethanol (1:1). The time of etching was 40 min and the current density was 60  $\text{mA}/\text{cm}^2$ . The free standing PSi films were obtained by lifting from the substrate after applying of a short pulse of the etching current 500  $\text{mA}/\text{cm}^2$ . Prior investigations the porous silicon films were air-dried for one week. The mesoporous silicon was obtained using similar procedure on heavily boron-doped p-type silicon wafer, with the specific resistivity of 1-5  $\text{m}\Omega\cdot\text{cm}$ , (100)-oriented. Silicon nanowires (SiNWs) were obtained by using metal-assisted chemical etching of c-Si wafers of p-type, boron doped, 1-10  $\Omega\cdot\text{cm}$ , (100)-oriented (see for details Ref. [11]). In order to investigate stability of Si nanostructures in water the corresponding powders were suspended in water. Films of microporous silicon were grinded in water or in aqueous solution of dextrane. Si NPs, which were prepared by microwave induced decomposition of silicon tetrafluoride [12], were mixing with water or aqueous dextrane solution followed with drying in air.

## RESULTS AND DISCUSSION

Figure 1 shows typical XRD patterns for c-Si powder, SiNWs, meso- and micro- PSi in semi-logarithmic scale. It can be clearly seen that there is almost no difference in XRD patterns of c-Si and Si NWs within the detection limit about 0.01 deg. The XRD spectrum of SiNWs consists of peaks corresponding to the presence of silver (Ag) nanoparticles used during the synthesis. The amount of silver, estimated via the corundum numbers is  $2\pm 0.5$  mass %. The amount of amorphous phase corresponds to the background signal intensities, so the relative amount of amorphous oxide can be measured as a ratio between background signal and peak intensity.

Mean size of Si nanocrystals in micro- and meso-PSi can be estimated from the broadening of diffraction line by using the Scherrer equation:

$$d = \frac{K\lambda}{\Delta\theta\cos\theta}, \quad (1)$$

where  $\lambda$  is the wavelength of x-ray radiation ( $\lambda=0.154184$  nm, in our case),  $K$  is a dimensionless shape factor close to unity,  $\Delta\theta$  is the line broadening at half the maximum intensity (FWHM),  $\theta$  is the Bragg angle of the corresponding crystallographic plane.

According to Eq.1 the mean size of Si crystallites in micro-PSi and meso-PSi is 2.7-4.4 nm and 10-15 nm, respectively, which in accordance with the literature data for similar preparation conditions [1,2].

Figure 2 shows XRD spectra for Si NPs prepared by silane decomposition and c-Si powder (for comparison). The broadening of Si NPs lines allows us to estimate the nanocrystal mean sizes to be about 30-40 nm. The background of XRD spectrum of Si NPs indicates the presence of amorphous phases, which can be both amorphous Si and  $\text{SiO}_2$ .

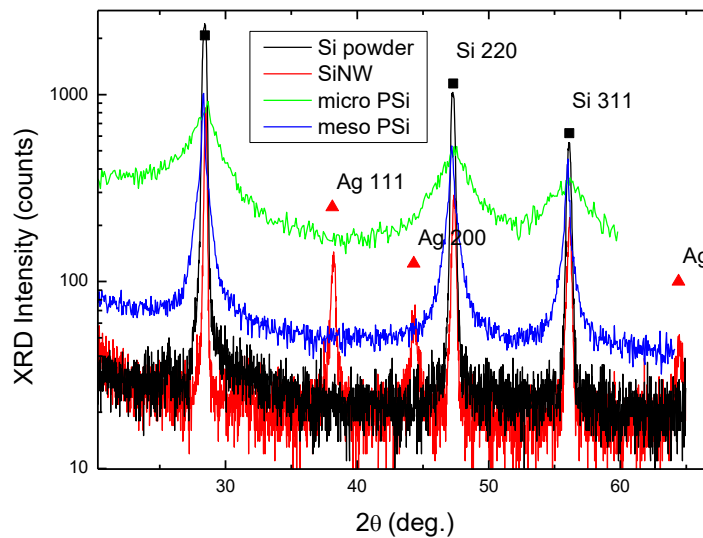


**Fig 1: XRD spectra of powders of c-Si, SiNWs, meso-PSi and micro-PSi. Black squares and red triangles indicate positions of the corresponding scattering angles for c-Si and crystalline silver from the XRD database.**

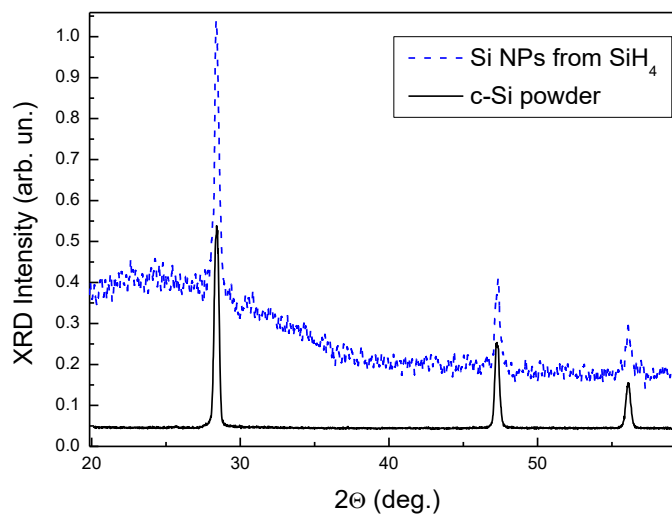


**Fig 2: XRD spectra of powders of Si NPs prepared by silane decomposition and c-Si (for comparison).**

According to Figure 3, the storage of Si NWs in water did not significantly change the XRD patterns, while the grinding of porous silicon in presence of water during 10 min cause significant change of XRD. It is known that micro-PSi can be oxidized by water [2], so the silicon peaks disappear and instead we can see increase of the background caused by the presence of amorphous silicon oxide.

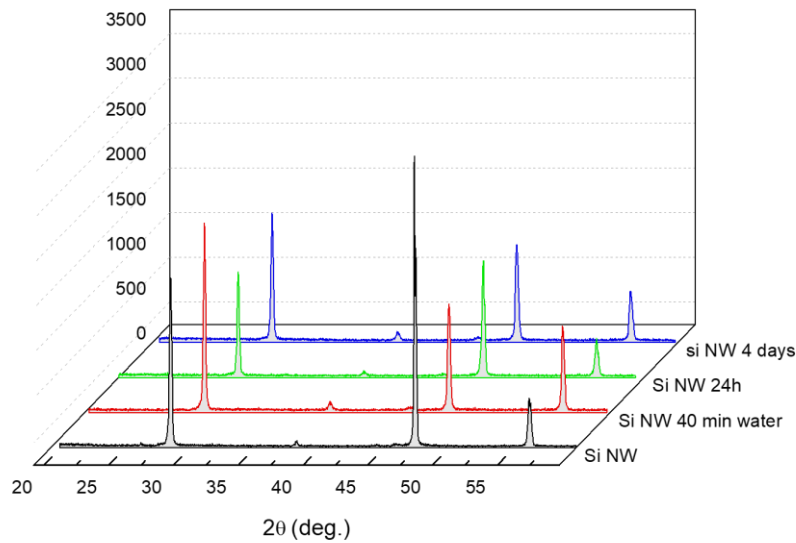


**Fig 3: XRD spectra of Si NWs before and after storage in water for different storage time.**

Assuming that the average thickness of oxide layer at the surface of silicon at room temperature without thermal treatment usually varies from 1 to 1.5 nm and taking in account the shape and size of the particles we can calculate the ratio between Si and SiO<sub>2</sub> phases. It can be expressed through the bond absorption for each type of particles. The ratio of background intensity (caused mainly by the presence of amorphous SiO<sub>2</sub>) and integral intensity of XRD silicon peak with maximum at 28.44° can be used to show the increasing amount of amorphous silica in nanostructures with decrease of their size. It allows us to propose the following expression for the ratio between XRD intensities and masses of Si and SiO<sub>2</sub> fractions:

$$\frac{I_{background}}{I_{peak}} \sim \frac{m_{SiO_2}}{m_{Si}} \quad (2)$$

Figure 4 shows the data calculated according Eq.2 versus the mean size of Si nanocrystals.

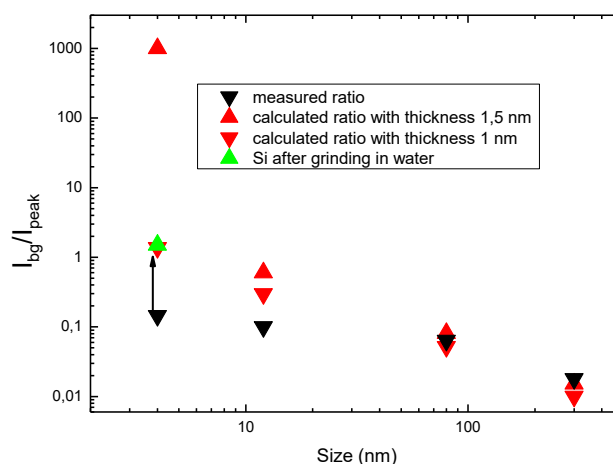


**Fig 4: Dependence of the ratio between the XRD background and intensities of the characteristic c-Si lines vs mean size of Si nanocrystals.**

Figure 4 shows that the decrease of size of Si nanocrystals results in an increase of the content of silica phase. Nevertheless, in case of relatively big nanostructures, the oxidation layer seems to correspond the model

of constant silica thickness, while in the case of porous silicon we can see that the particles are much less oxidized than they are supposed to be from the model of free-standing crystallites. That effect is probably caused by the complicated porous structure of the nanoparticles. That structure slows down the diffusion of oxygen. That effect also leads to the possibility of self-inflammation or even explosion of porous silicon during mechanical treatment. After grinding of PSi layer in water, we can observe the partial oxidation of the microporous silicon (green star in Fig.4) and formation of silicon oxide in amount equivalent to the formation of 1nm layer of silicon dioxide on each crystallite.

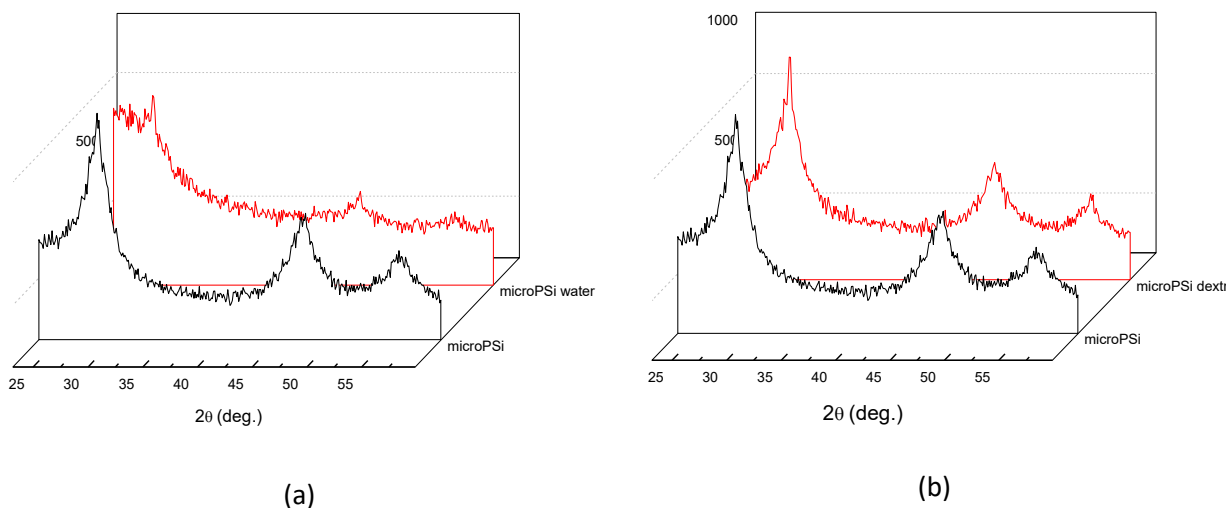


**Fig 4: (a) XRD spectra of micro-PSi before and after grinding in water: (b) the same spectra for micro-PSi treated in aqueous solution of dextrane.**

### CONCLUSION

The obtained results reveal a great potential of the x-ray diffraction technique for the determination of size of Si nanocrystals, amount of silicon oxide (after calibration) and it can be used to monitor the stability/degradation of silicon nanostructures in aqueous solutions. The performed measurements demonstrate the correlation between the nanocrystal size and the content of amorphous silica in different Si-based nanostructures. It was shown, that the fast oxidation of small Si nanoparticles occurred in water, but it could be slowed down by the dextrane coating. The obtained results can be used to monitor the dissolution rate of silicon nanostructures in aqueous media for various biomedical and sensor applications.

### ACKNOWLEDGMENTS

Authors acknowledge P.G. Sennikov for providing the samples of Si nanoparticles. The work was partially supported by the Russian Foundation for Basic Research (grant #16-02-00668). R.B.A. thanks the support of the PhD Program of Satpaev National Research Kazakh University.

### REFERENCES

- [1] Canham, L. T. (1990). *Appl. Phys. Lett.*, 57(10) 1046-1048.
- [2] Sailor, M. J. (2012). *Porous silicon in practice: preparation, characterization and applications*. Weinheim, Germany.
- [3] Wu, C., Crouch, C. H., Zhao, L., Carey, J. E., Younkin, R., Levinson, J. A., Karger, A. *Appl. Phys. Lett.*, 78(13) 1850-1852 (2001).
- [4] Halbwax, M., Sarnet, T., Delaporte, P., Sentis, M., Etienne, H., Torregrosa, F., Martinuzzi, S. (2008). *Thin Solid Films*, 516(20), 6791-6795.
- [5] Lin, V. S. Y., Motesharei, K., Dancil, K.P. S., Sailor, Ghadiri, M. R. (1997). *Science*, 278, 840-843.



- [6] Ahn, J.-H., Kim, J.-Y., Seol, M.-L., Baek, D. J., Guo, Z., Kim, C.-H., Choi, S.-J., Choi, Y.-K. (2013). *Appl. Phys. Lett.*, 102, 083701.
- [7] Erogbogbo, F., Yong, K. T., Roy, I., Xu, G., Prasad, P. N., Swihart, M. T. (2008). *ACS Nano*, 2, 873-878.
- [8] Park, J. H., Gu, L., Maltzahn, G. V., Ruoslahti, E., Bhatia, S. N., Sailor, M. J. (2009). *Nat. Mat.*, 8, 331-336.
- [9] Kabashin, A. V., Timoshenko, V. Yu. (2016). *Nanomedicine*, 11(17), 2247-2250.
- [10] Canham, L. T. (2007). *Nanotechnology* 18, 185704.
- [11] Timoshenko, V. Yu., Gonchar, K. A., Golovan, L. A., Efimova, A. I., Sivakov, V. A., Dellith, A., Christiansen, S. H. (2011). *J. Nanoelectr. & Optoelectr.*, 6(4), 519-524.
- [12] Vodopyanov, A. V., Golubev, S. V., Mansfeld, D. A., Sennikov, P. G., Drozdov, Y. N. (2011). *Rev. Sci. Instr.* 82, 063503.